2019 SCEC Proposal – Final Report

Toward Full Waveform Tomography Across California (Year 2)

Carl Tape, Principal Investigator
Geophysical Institute
University of Alaska Fairbanks
2156 N. Koyukuk Drive
Fairbanks, AK, 99775
Phone: 907-474-5456
Email: `ctape@alaska.edu`

Clifford Thurber, Principal Investigator
Department of Geoscience
University of Wisconsin-Madison
1215 W. Dayton St.
Madison, WI 53706
Phone: 608-262-6027, FAX: 608-262-0693
Email: `cthurber@wisc.edu`

Total amount of award:	$ 50,000
Amount awarded to UAF (Tape):	$ 25,000
Amount awarded to UW (Thurber):	$ 25,000

2019 SCEC RFP

Proposal Category:	B: Integration and Theory
SCEC Science Priorities:	4a, 3a, 3b

Overview and project personnel

Our project was proposed in fall 2018 and, with a no-cost-extension, continued through January 2021. Project personnel spanned two cycles of postdocs at UAF and UW. At UW, Avinash Nayak (now at LBNL) was succeeded by Ben Heath; at UAF, Vipul Silwal (now at IIT Roorkee) was succeeded by Julien Thurin. The project also included valuable participation from UVW PhD student Bryant Chow (pyatoa developer) and from UAF postdoc Ryan Modrak (seisflows developer).

The original statement of work included two objectives:

1. Refine iterative inversion workflow for adjoint tomography in California. Training across two different groups (UW, UAF) was a focus.

2. Apply our workflow to CVM-H15.1 with a small set of earthquakes. This was demonstrated for New Zealand earthquakes in *Chow et al.* (2020) and, in this report, partially demonstrated for CVM-H15.1.

Research products

1. Nayak and Thurber's efforts were published in *Nayak and Thurber* (2020).

2. The open-source adjoint tomography workflow used in this project was published in *Chow et al.* (2020). The software package is called pyatoa and is available from

   `https://github.com/bch0w/pyatoa`

3. Tools developed by Julien Thurin for model extraction from IRIS EMC and implementation into SPECFEM3D will be available either from within the SPECFEM3D software package (`https://github.com/geodynamics/specfem3d`) or from developmental repositories at UAF (`https://github.com/uafgeotools`).

For details on *Nayak and Thurber* (2020) or *Chow et al.* (2020), please see those published papers or the summaries in the interim report.

Improvements in the open-source workflow for adjoint tomography

1. Selection of target region and reference model. Archival and dissemination of tomographic models in California is a focus topic of the SCEC CVM TAG, which has held meetings in 2018, 2019, and 2020 (`https://www.scec.org/workshops/2020/cvm`). The primary SCEC CVMs (CVM-H15.1 and CVM-S4.26) are available from the UCVM software (*Small et al.*, 2017), which provides considerable flexibility for the user. SCEC is now looking toward the IRIS EMC (*IRIS*, 2011) to open the possibilities of users accessing many more tomographic models, all in in a uniform format (netcdf). To this end, the CVM TAG meetings recommended SCEC CME (*Jordan et al.*, 2003) provide a netcdf version of a CVM, for initial testing purposes, at the IRIS EMC. Thankfully this was achieved in Sept 2020:
   `http://ds.iris.edu/ds/products/emc-cvm_h_v15_1/`

   Julien Thurin wrote and adapted scripts to read the netcdf file and write it in the format needed for SPECFEM3D. The target region was a relatively small, 500 km x 400 km x 250 km region of southern California.

2. Hypocenters and origin times.
   Waveform-relocated hypocenters and origin times in southern California (*Hauksson et al.*, 2012) are updated on a quarterly basis (E. Hauksson, e-communication). These source parameters are sufficiently accurate for us to avoid introducing artifacts into the adjoint-based inversion, which targets periods 2 s and longer.

3. Estimation of moment tensors.
   Moment tensors were estimated by Julien Thurin using the open-source code MTUQ `https://github.com/uafgeotools/mtuq` developed by Ryan Modrak and Carl Tape. MTUQ uses the cut-and-paste method established by *Zhu and Helmberger* (1996), used in *Tape et al.* (2009) for the initial moment tensors, and recently adapted and applied in *Silwal and Tape* (2016); *Alvizuri and Tape* (2016); *Alvizuri et al.* (2018).

4. Meshing provides the discretization of the 3D tomographic model needed for the wave propagation solver SPECFEM3D. SPECFEM3D provides a fast, simple meshing approach (*Komatitsch et al.*, 2004) that accommodates topography and internal discontinuities such as the Moho. The hexahedral mesh we used is shown in Figure 1c.

5. Forward simulations were performed by Julien Thurin using SPECFEM3D. Example comparison of data and synthetics are shown in Figure 1d-f.

6. We did not perform any iteration on the tomographic model, as proposed. At the time of this report (March 2021), pyatoa was under development to upgrade seisflows by June 2021. PIs Tape and Thurber opted to invest the limited allocated postdoc time toward developing early portions of the workflow.

Training development

Postdoc Ben Heath has been working with Carl Tape of the University of Alaska Fairbanks (UAF) and his research group on learning to do the wavefield simulations for our new velocity model in comparison to the SCEC CVMs.

Over the summer, Tape trained Heath on running simple, introductory, block forward wavefield models using SPECFEM3D on the UAF high-performance computing (HPC) cluster "chinook". Heath gained valuable skills, learning to both run the waveform code (SPECFEM3D) and work in HPC environments. The setting provided by Tape and his research group additionally provided an excellent example of how to foster efficient learning practices in computationally complicated environments. Specifically, the group developed a number of different routines/workflows that enabled novice users to quickly learn to run basic, block waveform models on high-performance computers.

At UAF, Thurin developed the necessary files to run example waveforms for a single event located in Southern California. These files included the seismologically necessary information (e.g. tomography model, station list, event meta data, topography data) as well as computationally necessary information (e.g. number of nodes and time lengths to submit in job requests when using the supercomputer). This framework enabled Heath to easily run and recreate Thurin's work on the UAF supercomputer. This experience provided Heath with an example of how to run waveforms through a geologically realistic model in a region of interest.

Summary

Significant progress has been achieved towards the goal of a complete, open-source, full-waveform tomography workflow. An improved procedure for processing of ambient noise cross-correlation data has been developed. A new model for the central California region has been determined using a joint inversion of body-wave and surface-wave data.

Further development and applications of the full-waveform tomography workflow is needed. The improved ambient noise processing method also requires further evaluation, but it shows potential for broad improvement of ambient noise data processing. The new central California seismic velocity model needs to be validated with forward wavefield simulations and compared against the effectiveness of the SCEC CCA model in predicting observed waveforms.

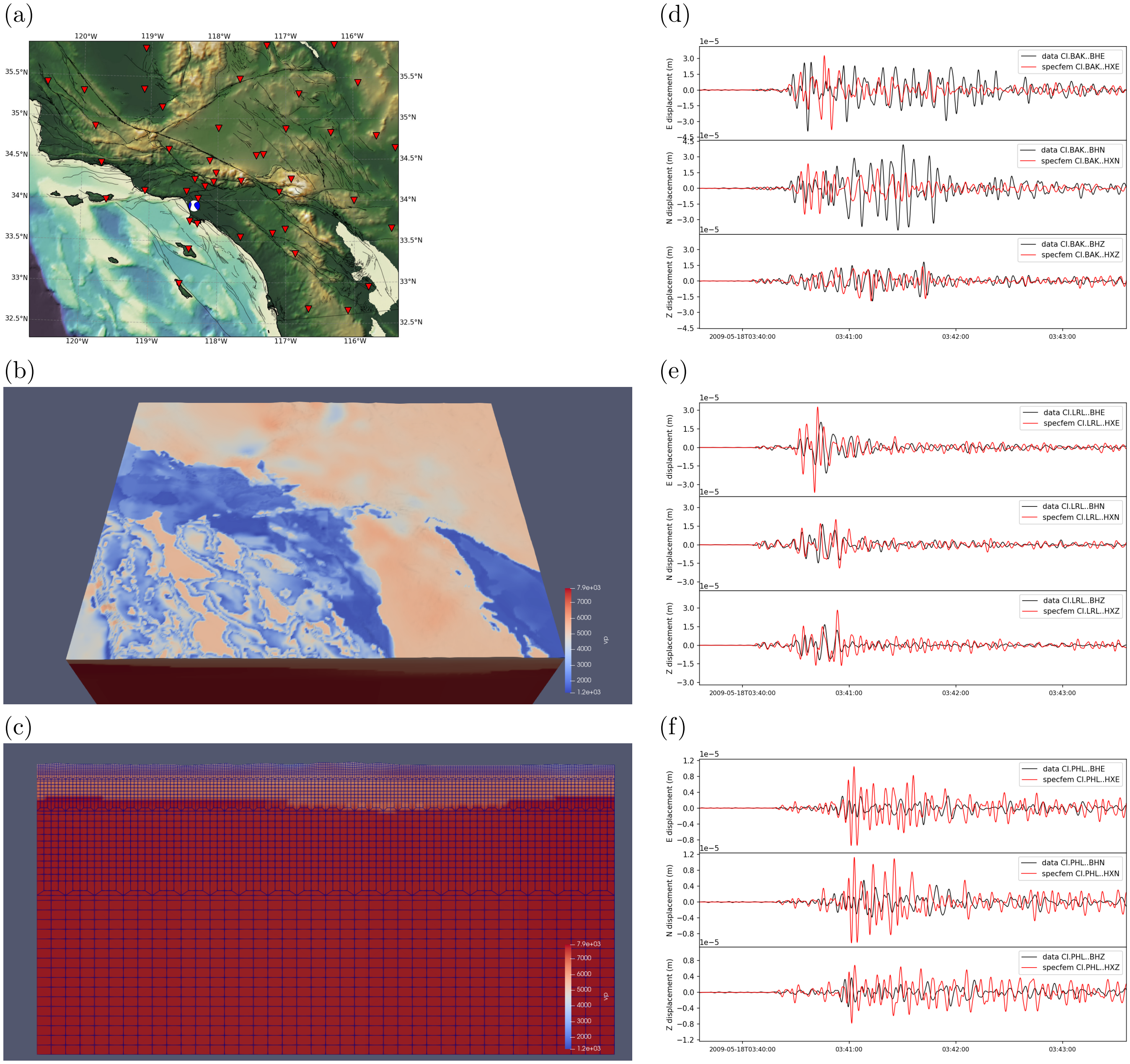

Figure 1: Example components of the workflow. (a) Choice of 500 km x 400 km simulation domain, along with CI stations. (b) 3D view of CVM-H15.1 obtained from the netcdf file at the IRIS EMC. (The default color scale shows red fast and blue slow.) (c) Side view of the unstructured hexahedral finite-element mesh used for 3D wavefield simulations in SPECFEM3D. Note the three doubling layers, where elements double in length from the shallower to deeper layer. Larger elements are used for higher-velocity mantle material in order to efficiently use the available computational resources. (d)-(f) Example seismogram comparisons (red synthetic, black data) for stations BAK (Bakersfield), LRL (Laurel Mt.; near Garlock), and PHL (Park Hill; near San Luis Obispo), filtered 3–9 s. BAK typifies a region where the 3D model does not capture the true 3D heterogeneity. LRL shows good fits to relatively simple waveforms, exhibiting bedrock structure. PHL shows a case where the synthetic amplitudes are too high, possibly due to unreasonably slow velocity values in the model.

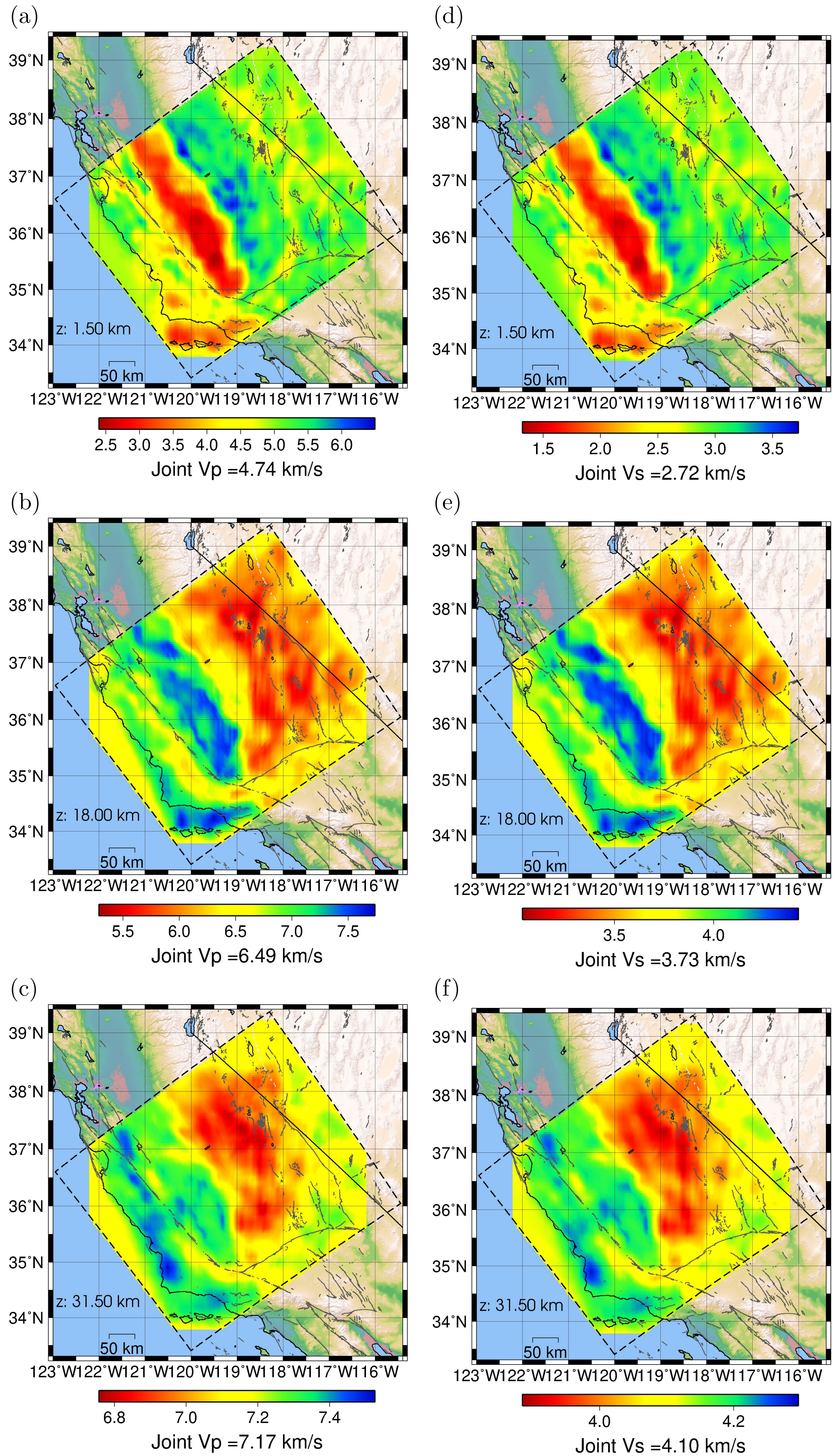

Figure 2: Depth slices through the joint inversion model from body waves, Rayleigh waves, and Love waves. (a-c) Depths of 1.5, 18, and 31.5 km (bsl) for Vp. (d-f) Depths of 1.5, 18, and 31.5 km (bsl) for Vs.

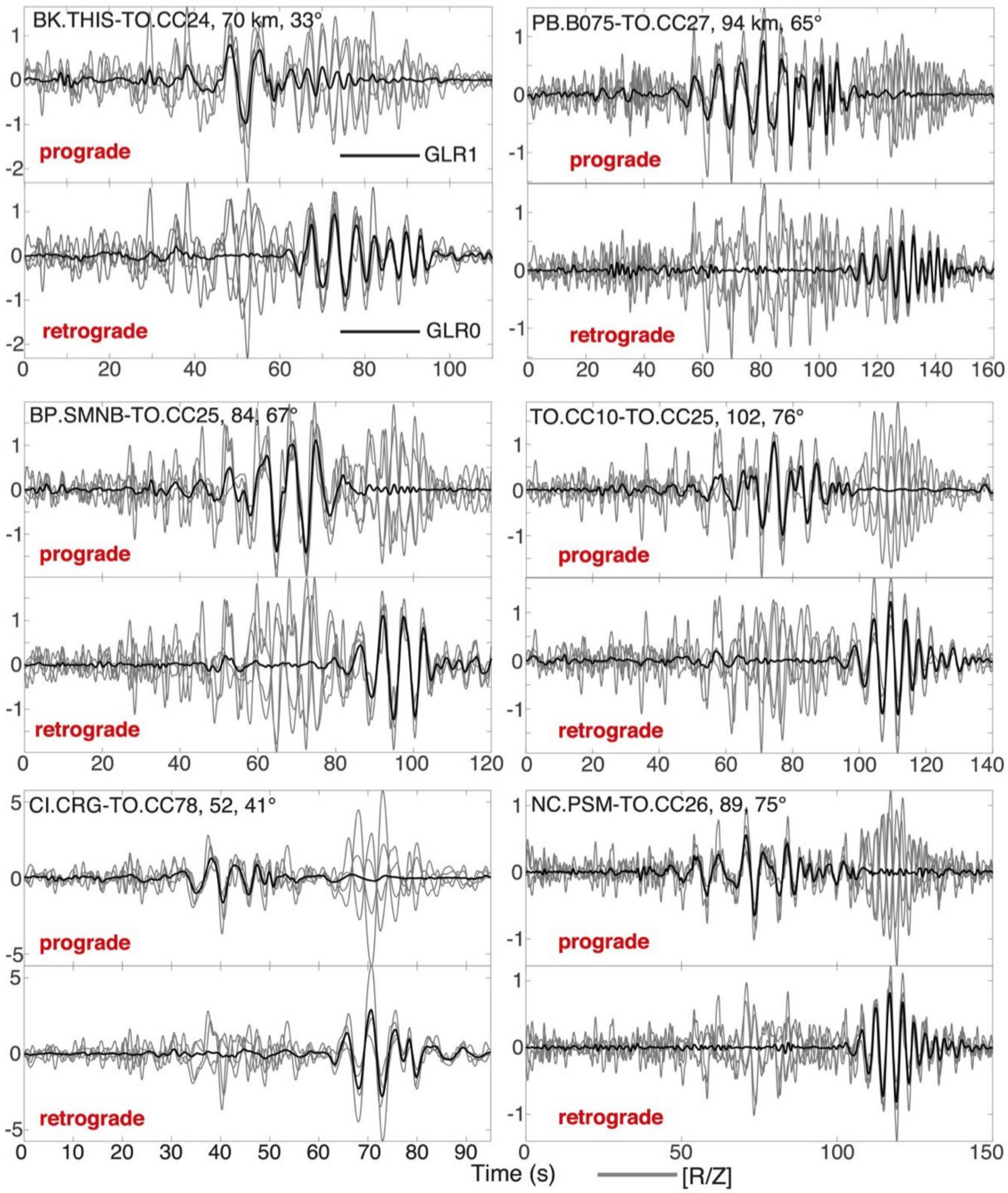

Figure 3: Excerpt from *Nayak and Thurber* (2020). Each pair of plots shows [R/Z] component noise cross-correlations (gray waveforms) that are phase corrected assuming prograde (top plot) and retrograde (bottom plot) elliptical particle motion and stacked by phase-weighted stacking in the t-f domain using the S-transform (black waveforms; top plot: GLR1 and bottom plot: GLR0). Network and station names for the station pair, inter-station distance (km), and azimuth (°) are indicated on each plot. Y-axis units are proportional to displacement response for an input step force. These waveforms are bandpass filtered in the range 0.07–0.8 Hz. In each pair of plots, the RR and ZR components are unchanged, and the RZ and ZZ components are flipped. Note the clear emergence of the earlier first higher mode Rayleigh wave and suppression of the fundamental mode Rayleigh wave on the prograde stacks and the opposite for the retrograde stacks.

References

Alvizuri, C., and C. Tape (2016), Full moment tensors for small events ($M_{\mathrm{w}} < 3$) at Uturuncu volcano, Bolivia, *Geophys. J. Int.*, *206*, 1761–1783, doi:10.1093/gji/ggw247.

Alvizuri, C., V. Silwal, L. Krischer, and C. Tape (2018), Estimation of full moment tensors, including uncertainties, for nuclear explosions, volcanic events, and earthquakes, *J. Geophys. Res. Solid Earth*, *123*, 5099–5119, doi:10.1029/2017JB015325.

Chow, B., Y. Kaneko, C. Tape, R. Modrak, and J. Townend (2020), An automated workflow for adjoint tomography—waveform misfits and synthetic inversions for the North Island, New Zealand, *Geophys. J. Int.*, *223*, 1461–1480, doi:10.1093/gji/ggaa381.

Hauksson, E., W. Yang, and P. M. Shearer (2012), Waveform relocated earthquake catalog for southern California (1981 to June 2011), *Bull. Seismol. Soc. Am.*, *102*(5), 2239–2244, doi:10.1785/0120120010.

IRIS (2011), Data Services Products: EMC, A repository of Earth models, `https://doi.org/10.17611/DP/EMC.1`.

Jordan, T. H., P. J. Maechling, and the SCEC/CME Collaboration (2003), The SCEC Community Modeling Environment: An information infrastructure for system-level earthquake science, *Seismol. Res. Lett.*, *74*(3), 324–328, doi:10.1785/gssrl.74.3.324.

Komatitsch, D., Q. Liu, J. Tromp, P. Süss, C. Stidham, and J. H. Shaw (2004), Simulations of ground motion in the Los Angeles basin based upon the spectral-element method, *Bull. Seismol. Soc. Am.*, *94*(1), 187–206, doi:10.1785/0120030077.

Nayak, A., and C. H. Thurber (2020), Using multi-component ambient seismic noise cross-correlations to identify higher mode Rayleigh waves and improve dispersion measurements, *Geophys. J. Int.*, *222*, 1590–1605, doi:10.1093/gji/ggaa270.

Silwal, V., and C. Tape (2016), Seismic moment tensors and estimated uncertainties in southern Alaska, *J. Geophys. Res. Solid Earth*, *121*, 2772–2797, doi:10.1002/2015JB012588.

Small, P., D. Gill, P. J. Maechling, R. Taborda, S. Callaghan, T. H. Jordan, K. B. Olsen, G. P. Ely, and C. Goulet (2017), The SCEC Unified Community Velocity Model software framework, *Seismol. Res. Lett.*, *88*(6), 1539–1552, doi:10.1785/0220170082.

Tape, C., Q. Liu, A. Maggi, and J. Tromp (2009), Adjoint tomography of the southern California crust, *Science*, *325*, 988–992, doi:10.1126/science.1175298.

Zhu, L., and D. Helmberger (1996), Advancement in source estimation techniques using broadband regional seismograms, *Bull. Seismol. Soc. Am.*, *86*(5), 1634–1641.